Establishing a Standardized Test Method for Evaluating Space Suit Gloves Thermal Performance at Lunar South Pole Temperatures

Morgan Abney[1], Tim Brady[2], Danielle Morris[3], Sara Wilson[4]
NASA Engineering and Safety Center, Langley Research Center, Hampton, VA 23666

Noah Andersen[5]
HX5, LLC (JETS 2), Houston, TX, 77058

Bruce Conger[6]
Amentum (JETS 2), Houston, TX, 77058

Robert J. Jones[7], Shane McFarland[8]
Leidos, Aegis Aerospace / KBR HHPC / NASA Johnson Space Center, Houston, TX 77058

Wade Smith[9], Lori Shiraishi[10]
NASA Jet Propulsion Lab, La Canada Flintridge, CA 91011

Anthoney Shawn Deaton[11]
Textile Protection and Comfort Center, Raleigh, NC 27695

Andrew Funk[12]
Wells Lamont Industrial, Skokie, IL 60077

The Artemis space suit glove environmental protection garment (EPG) will be the first line of protection used to shield the crewmembers' hands from the thermal extremes encountered during Lunar south pole extravehicular activity (EVA). The Artemis missions will encounter more extreme thermal environments than those experienced during Apollo or aboard the International Space Station, presenting significant challenges for the development, verification, and validation of gloves. There are no standardized tests designed to evaluate the thermal protection of space suit gloves at the lunar temperature extremes found in the permanently shadowed regions (PSR). Also, there is insufficient data on state-of-the-art glove performance in a lunar PSR from which to compare new designs. Therefore, it is necessary to design tests to evaluate glove thermal performance to determine if they are sufficient to meet new, challenging requirements. This paper focuses on the development of a test procedure to characterize lunar EVA glove EPGs thermal conductivity at increasing colder temperatures down to Lunar PSR equivalent temperatures and then using that procedure to collect data on the Phase VI Glove. The test utilized a Thermal Hand System (THS), a thermally controlled manikin hand outfitted with a suite of sensors, and three thermal fluid loops to simulate human blood flow. The data were used to correlate a thermal math model of the glove which

[1] ECLSS Technical Fellow, NASA Engineering and Safety Center, C104, Marshall Space Flight Center, AL.
[2] NESC Integrator, NASA Engineering and Safety Center, C102, Johnson Space Center, TX.
[3] NESC EVA and Human Mobility Deputy, Marshall Space Flight Center, AL.
[4] NESC Statistician, NASA Engineering and Safety Center, C102, Langley Research Center, Hampton, VA.
[5,6] Thermal Analysis Engineer, 224 Bay Area Blvd./JE-5EA.
[7,8] Spacesuit Engineer, Crew and Thermal Systems Division, NASA Johnson Space Center, Houston, TX.
[9,10] CITADEL Chamber Laboratory Manager, NASA JPL, La Canada Flintridge, CA.
[11] Operations Director, Textile Protection and Comfort Center, Raleigh, NC 27695.
[12] Senior R&D Laboratory Manager, Wells Lamont, Skokie, IL.

was ran real-time during testing to help predict initial conditions and thermal response times. Following correlation of the thermal glove model, new glove curves were generated. The glove curves can be used to determine the permissible touch durations at different environment temperatures including lunar PSR temperatures.

Acronyms and Nomenclature

ASTM	=	American Society of Testing and Materials
C	=	Celsius
CITADEL	=	Cryogenic Ice Transfer, Acquisition Development, and Excavation Laboratory
COS	=	Committee on Standards
EPG	=	Environmental Protection Garment
EVA	=	Extravehicular Activity
F	=	Fahrenheit
HITL	=	human-in-the-loop
ISS	=	International Space Station
JPL	=	Jet Propulsion Laboratory
K	=	Kelvin
LEO	=	low Earth orbit
LN2	=	Liquid Nitrogen
MLI	=	Multi-layered Insulation
MP	=	Metacarpophalangeal
NESC	=	NASA Engineering and Safety Center
PSR	=	permanently shadowed region
THS	=	Thermal Hand System
TMG	=	Thermal Micrometeoroid Garment

I. Introduction

Due to the short timeline to the Artemis III mission, currently planned for 2027, and the criticality of providing lunar EVA spacesuits, NASA has undertaken an effort to address three key obstacles to producing a spacesuit glove that is sufficiently durable to meet the needs of the Artemis mission. These obstacles include:

1. No consistent/standardized testing has been defined to evaluate the durability of gloves for the extreme lunar environments.
2. No baseline lunar thermal performance data exist on the Phase VI gloves from which to compare new designs.
3. Phase VI glove fabrics are unlikely to be sufficient to meet lunar abrasion, cut resistance, and thermal requirements.

NASA space suit engineers, material experts, and test personnel were assembled and the effort to address these obstacles was divided into several tasks. Three previous papers detail the results of two of the tasks. They include: ICES-2023-37 “Establishing Standardized Test Methods for Evaluating Space Suit Gloves” which details the development of a new standardized test procedure (the rotary tumbler) for vetting candidate fabrics for use in Extravehicular Activity (EVA) gloves and using the procedure to compare fabric performance against lunar conditions, ICES-2024-50 “Validation Testing and Statistical Analysis of the Rotary Tumbler Fabric Abrasion Method,” which details how the development of the tumbler test necessitated conducting a validation test and statistical analysis to define its repeatability (variability) and the repeatability limit (maximum difference), and ICES-2024-52 “Establishing a Standardized Test Method for Evaluating the Cut Resistance of Space Suit Glove Fabrics,” which focused on the development of a test procedure to characterize the cut resistance of lunar EVA glove fabrics at cryogenic temperatures using a modified American Society of Testing and Materials (ASTM) standardized test method. This paper details the efforts of the final task set out to develop a test procedure for characterizing the thermal performance of a glove assembly and then using that procedure to collect glove data at temperatures equivalent to lunar PSR.

II. Test Approach

A. Overview

Previous ISS glove human-in-the-loop (HITL) thermal tests used multiple human test subjects in a partial vacuum chamber inserting their hands and forearms into EVA gloves in a full vacuum chamber to take various hand and glove temperature measurements in radiative and direct contact environments. It produced data from various EVA gloves that were thermally tested to determine maximum exposure duration and touch contact limits on extremely cold or hot objects representing what would be encountered during a low Earth orbit (LEO) EVA.[1] Testing evaluated performance with and without active glove heating. The test data were used to correlate a thermal math model of the glove, which produced thermal performance curves that are used to plan EVA objectives.

Historical testing with the ISS glove did not achieve lunar temperatures resulting in a gap in data needed to quantify the risk of using heritage ISS gloves in a lunar environment and for iterative lunar glove design work. Therefore, the approach taken for this assessment targeted a non-human test protocol that drove the need to develop a custom thermal manikin hand system to use as an analogue. The NASA team worked with Thermetrics, LLC to develop a bespoke human analogue solution that could be used to mimic the HITL glove protocols used to establish the touch temperature limits of the ISS EVA gloves.

Previous testing determined the thermal performance of the Phase VI gloves for the ISS environments. Lunar PSR environments are outside of this range on the cold side extending to as low as 48 K. Therefore, this task focused on testing at the lower end PSR temperatures to determine the limits of the glove in radiation and grasp conditions. A thermal vacuum chamber capable of reaching 48 Kelvin (K) was identified, and a modified protocol was established to standardize the method for collecting the required thermal data from a pressurized glove installed onto the manikin hand. For comparison purposes, test point parameters were designed and controlled similar to previous testing of the Phase VI Glove.

The test protocol was designed to determine several sets of data. First, a correlation between the previous data collected using the HITL method to the new method using the human analogue manikin hand. Next, the maximum exposure duration (radiative case) of the Phase VI Glove at decreasing temperatures approaching 48 K (or lowest chamber temperature) at vacuum (10^{-4}–10^{-8} Torr) with and without glove heaters. Then, the maximum touch duration (contact case) of the glove in three locations (palm, fingers, fingertips) with a predefined pressure at decreasing temperatures approaching 48 K at vacuum (10^{-4}–10^{-8} Torr) with and without glove heaters. Finally, a statistical analysis was conducted on the data to determine the repeatability of results using the same Phase VI glove assembly and the variability of results using multiple Phase VI glove assemblies.

The newly developed Test Plan defines a procedure for testing the thermal performance characteristics of a Phase VI Glove Thermal Micrometeoroid Garment (TMG) in radiation, grasp, and high-force grasp positions at increasingly colder temperatures until reaching 48 K. The test utilizes a thermal hand system (THS), a thermally controlled manikin hand outfitted with a suite of sensors, and three thermal fluid loops to simulate human blood flow (see Figure 1). Additional information about the design of the hand is found in ICES-2025-412. The glove is installed over the THS and both items are mounted to a set of sealed, extendable arms installed in the Cryogenic Ice Transfer, Acquisition Development, and Excavation Laboratory (CITADEL) thermal vacuum chamber at Jet Propulsion Laboratory (JPL) (see Figure 1). Wilson seals enable the shafts to move through a vacuum boundary by using flexible, preloaded sealing elements that maintain continuous contact with the shaft surface. These seals accommodate rotational and/or linear motion while preventing gas ingress, ensuring the integrity of the vacuum environment. The chamber uses helium and rapid expansion gas valves to cool the floor of the chamber. When defined temperature set points are achieved, the arms are used to manipulate the THS/glove system into the chamber where it is pressed into a thermally conditioned grasp object on the floor of the chamber (see Figure 1). Using embedded sensors (heat flux and temperature), the procedure is utilized to collect data on the glove (in this instance, Phase VI) performance. A Load Lock allows change out of the test articles while maintaining the conditioning of the main chamber.

For this task, the data were used to correlate an existing thermal math model of the glove. The math model is used to generate touch limiting temperature curves for the entire range of temperatures that could be encountered during an Artemis EVA. This model will then be used to help plan crew activity.

Touch locations on the gloves were chosen to represent areas that are compressed when grasping an object.

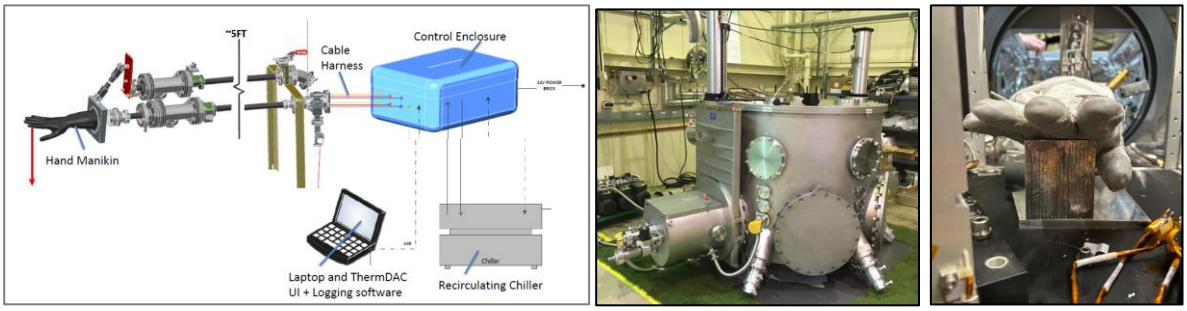


Figure 1. EVA glove thermal test setup. (Left) The Thermal Manikin Hand System installed into the EVA glove and provided heating and data. (Center) The CITADEL Chamber at JPL can reach 48K and was used for testing. (Right) The Phase VI Glove was installed on the THS, inserted into the chamber, and pressed into a conditional grasp object.

Because the glove is stiff when pressurized, it would be difficult to uniformly compress all areas concurrently. Therefore, the test isolates these areas to ensure worst case data (i.e., all compressive force in one area) are captured. This method simplifies the movement required of the THS. Additionally, the glove material ply-ups are not uniform, and the selected areas have unique constructions. Testing in these areas provided higher-fidelity thermal performance defined by the thermal resistance of the layups in these areas.

B. Glove Test Articles

Three Phase VI glove TMGs, all size 6C3, were used for this testing. One was the RTV 157 style (used from 1998 to 2008) and the other two were the 3145 style (used from 2008 to present) and were denoted as 3145A and 3145B for the duration of the testing. These TMGs were available at the time of testing, in good condition, and of matching sizes which simplified testing for repeatability.

Thermocouples were used to monitor the temperature of the glove TMG in conjunction with combined heat flux and thermocouples in the thermal hand. The sensor tips are required to be small to minimize the impact of the instrumentation on the conductance pathways. For the exterior of the TMG, the sensors were attached to the surface of the RTV pads using a thin layer of RTV over the thermocouple. For the interior of the TMG, they were sewn in place. For the thermal hand, the sensors were embedded in the hand mold at the surface.

There were 15 locations for temperature and heat flux measurements located in areas with the highest topology comparatively. This ensured that the temperature data were collected from the locations with the greatest compression between the gloved thermal hand and the grasp object. Each location had three temperature and one heat flux measurements with the tips of the sensors stacked on top of each other at the hand, between the glove restraint (internal TMG), and on the outside of the glove TMG.

C. Test Matrix, Test Conditions, Test Termination Criteria, Repetitions and Schedule

The test matrix focused on five unique chamber temperature set points that were targeted for data collection. Temperature targets were 200 K (–100°Fahrenheit [F]), 172 K (–150°F), 158 K (–175°F), 100 K (–280°F), and 48 K (–373°F). The first three set point temperatures mimic the chamber set points from previous glove testing. The last two set points are defined by the Artemis requirements.[2,3] The temperature of the test chamber and grasp object were designed to be nearly identical because the grasp object was thermally tied directly to the chamber cold plate and a cryocooler head via copper rope.

Radiation, touch point, and heater state test points were grouped together into “Temperature IDs” corresponding to the critical chamber temperature setpoints. The test point conditions followed a modified version of previous (1990s) HITL glove thermal test point matrix with three exceptions. First, high-pressure touch points were eliminated from the matrix due to limitations on the mechanical loads the test setup could provide. Second, radiation conditions were conducted first in the test sequence, rather than last. Finally, additional radiation tests were added to provide more correlation data to the Thermal Math Model.

Testing was performed on two versions of the glove with the 3145 style RTV (3145A and 3145B) and one version of the glove with the 157 RTV. The number of test point repetitions is shown in Table 1.

A significant change from the planned test matrix was due to a sensor alignment issue that is discussed in Section IVB. This issue resulted in all planned fingertip and finger test points being combined into "Finger" test points. All Finger test points were run at the same contact pressure, and test points were run with and without heaters for all temperature targets except for 200 K where test points were performed without heaters. This exception is in line with the original test matrix that had no test points planned with heaters on for the 200 K tests.

At the warmer temperature test points (200 K, 172 K, and 158 K), the water flowing through the manikin palm and finger regions was controlled to 27°Celsius (C; 80.6°F) to more closely simulate conditions of the 1998 HITL test.[1] During 1998 HITL testing, the initial hand temperature at the start of the test point varied case to case, but in general the hand temperature was near 27°C (81°F). For the colder temperature test points (100 K and 48 K), the water/glycol flowing through the manikin hand was controlled to 37°C (98.6°F). Based on results from early testing and analysis, it was predicted that at these cold conditions, a 27°C (80.6°F) water setpoint would result in finger contact test points shorter than a minute. Since longer duration test results would yield more valuable data for model correlation and better assessment of glove thermal performance, the higher water temperature was utilized during the 100 K and 48 K test points.

Test points were terminated when the restraint (internal TMG) sensor reached –30°C (–22°F) or when the test point time limit was reached, whichever came first. The time limit for radiation and nominal pressure palm test points was 15 minutes. A time limit of 10 minutes was used for the remaining test points.

Over the course of 25 days, each TMG was installed on the test apparatus and data collected with a series of repeating Temperature IDs to be able to compare data sets and establish the statistical significance of the changing variables. The chamber temperature was controlled in a way to quickly get repetitions at warmer Temperature IDs, changing out TMGs using the load lock, and then allowing the chamber to achieve its coldest temperatures and repeating colder Temperature IDs.

III. Thermal Analysis Approach

A. Model Description

The thermal glove model was developed using the Systems Improved Numerical Differencing Analyzer/Fluid Integrator computer code initially developed by NASA. The model breaks the hand/glove assembly into an array of numerous nodes and solves conservation of energy equations on this system. The hand is broken into eight separate sections (Palm, Metacarpophalangeal (MP) Joint, Middle Finger, Middle Fingertip, Index Finger, Index Fingertip, Thumb, Thumb tip). The ring and little finger are not present in the model (see Figure 2). It is assumed that the little and ring fingers will behave similarly to the index and middle fingers, respectively. Each of these sections is broken into three regions (palm, side, and back). Finally, within each of these sections, nine nodes represent the stack up of layers in the hand and glove. The conductance between the nodes in the model is based on test data and can be adjusted to correlate the model.

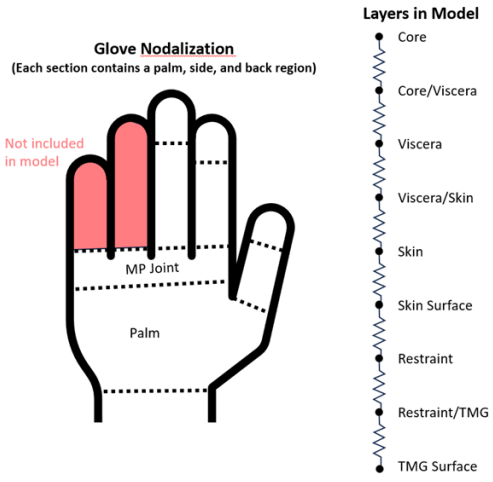


Figure 2. Glove/hand model.

B. Model Correlation

The model is correlated to test data by adjusting the conductance values (G) between the glove layers based on test data. The test was designed so that each sensor location has temperature sensors on the skin, interface between restraint and TMG, and external TMG surface. Additionally, the skin has a heat flux sensor. Since all sensors are aligned and there is minimal conduction of heat expected tangentially through the glove, a thermal conductance across each layer can be computed using

$$G_{i,skin\rightarrow res} = \frac{q_i'' \cdot A_i}{T_{skin,i} - T_{res,i}}$$

Where $G_{i,skin\rightarrow res}$ is the conductance between the skin and restraint in section i, q_i'' is the measured heat flux in section i, A_i is the total area of the skin in section i, $T_{skin,i}$ is the measured skin temperature, and $T_{res,i}$ is the measured restraint temperature. This conductance is plugged into the thermal model to represent the conductance between the 'skin surface' and 'restraint/TMG' layer as shown in Figure 2. This approach was also used to compute the conductance from the Restraint to the outside of the glove (using $T_{res,i}$ and $T_{TMG,i}$), and the glove to the environment (using $T_{TMG,i}$ and T_{env}).

C. Glove Curve Update

Following correlation of the thermal glove model, a glove curve was generated. The glove is used to determine the permissible touch durations at different environment temperatures. The glove curve was generated in a similar method to the glove curve generated in the initial testing of the Phase VI glove[1] and will be discussed more in the results section.

IV. Test Results

A. Test Point Durations

Table 1 shows the durations for each test point run in this test series. As mentioned in Section IIIC, test points were terminated when the restraint (internal TMG) sensor reached –30°C (–22°F) or when the test point time limit was reached, whichever came first. The time limit for radiation and nominal pressure palm test points was 15 minutes. A time limit of 10 minutes was used for the remaining test points. From initial inspection, the biggest, unexpected result was the coldest temperature test points (48K) resulting in longer test points than warmer temperatures. This was found to be a result of the chamber pressure and will be discussed in the next section. The other preliminary finding from this table was little differences in test point duration across different gloves, contact pressures, or glove heater status. While the test point duration begins to indicate the performance of the gloves, more extensive thermal analysis was needed to completely quantify the glove performance.

Table 1. Test point durations (minutes).

Temp	Case	3145A						3145B			157		
200 K	Radiation	20.8	25.1					30.5	24.7		16.7	16.8	
	Palm (Nom)	11.7	12.7					12.7	15.8		15.3	14.0	15.3
	Palm (Hi)	10.7	10.9					11.5	10.8		10.8	10.6	10.4
	Finger (NoQ)	9.7	10.1					10.4	5.5		4.4	9.6	5.6
172 K	Palm (Nom)	8.3	8.1					8.6	8.8		9.8	8.9	9.8
	Palm (Hi)	7.9	7.7					8.3	7.8		8.4	10.2	8.9
	Finger (NoQ)	7.3	4.8					2.8	3.3		3.7	4.4	4.8
	Finger (Q)	5.0	5.1					3.1	3.1		2.1	4.2	4.3
158 K	Radiation	9.1	8.9					9.7	9.1		14.5	12.1	9.4
	Palm (Nom)	7.6	7.2					7.6	7.5		8.6	7.9	8.8
	Palm (Hi)	7.3	7.4					6.9	6.4		7.3	7.9	8.1
	Finger (NoQ)	2.7	3.1					2.9	3.1		2.5	2.1	2.5
	Finger (Q)	3.7	3.1					2.7	3.5		2.6	2.5	2.7
100 K	Radiation	8.6						8.3			8.8		
	Palm (Nom)	8.6						6.6			5.9		
	Palm (Hi)	8.6						5.3			6.4		
	Finger (NoQ)	1.9						2.4			1.4		
	Finger (Q)	2.2						3.2			2.7		
48 K	Radiation	13.8	12.6	12.2	13.4	13.0	13.5	13.5	12.5	12.5	13.9	13.7	12.7
	Palm (Nom)	11.9	11.7	11.6	12.5	12.3	10.4	12.2	11.2	11.2	10.7	11.0	9.8
	Palm (Hi)	10.5	10.4	11.0	10.5	10.5	10.5	10.6	10.7	10.8	10.6	10.3	10.6
	Finger (NoQ)	4.3	5.6	3.8	4.3	5.4	4.9	7.6	7.5	10.3	3.8	1.8	2.0
	Finger (Q)	4.0	4.2	4.2	3.5	4.3	2.6	10.1	7.5	10.4	4.0	3.1	2.6

Orange entries indicate test points that were terminated due to the time limit being met, not a temperature limit. “Nom” indicates nominal pressure, “Hi” indicates high pressure, “NoQ” indicates no glove heaters were used during testing, and “Q” indicates glove heaters were on during the test.

B. Anomalies

1. Data Dropout During Testing

During the test series, there were some sensors that frequently gave erroneous data. The THS sensors were initially calibrated at the vendor prior to hand delivery. However during the test series there were some anomalies that appeared. In some instances, the data would be incorrect for the complete duration of the test, while in other instances, the data would sporadically cycle between erroneous values and values that appear to be accurate. For this data analysis, on test points where the sensor produced erroneous values, the sensor results were excluded for the full duration of the test point.

2. Alignment Issues

Another issue in data acquisition and sensor performance was a result of the fit of the manikin hand within the glove. For all three glove TMGs, with the exception of the thumb, the manikin hand did not reach the end of the glove, resulting in a gap between the end of the fingertip and the glove. This resulted in colder temperatures at the tips of the gloves and misalignment of sensors (See Figure 3). Computation of glove conductance requires alignment of the sensors in the hand to the sensors in the glove. As a result of the alignment issues, the glove sensors did not align with the hand sensors at the fingertip and finger locations (subscripts 1 and 2, respectively, in Figure 3). Fortunately, the fingertip sensors of the hand aligned with the finger sensors in the glove. For this reason, conductance computations were still possible in the fingers. This alignment was verified through positional calibration testing on the fingers of the glove.

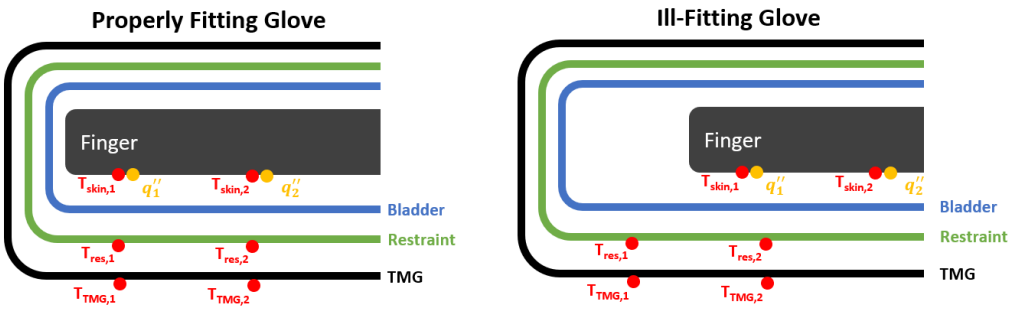


Figure 3. Comparison of a properly fitting glove to ill-fitting glove.

3. Nonuniform Contact

Another issue with testing was maintaining a uniform contact and pressure across all fingers. When a human test subject grasps an object, they are able to independently control the grasp pressure of each finger to give uniform pressure. By contrast, the manikin hand is a rigid structure with no ability to independently adjust the pressure of each digit. Efforts were made to design and redesign the grasp object so that a proper contact could be made with each finger. This was achieved on the index and middle finger. However, designing a repeatable grasp object that consistently contacts the manikin hand proved difficult. As a result of the rigid structures of the hand and grasp object, test points typically showed variable heat flux across different sensors, likely as a result of nonuniform contact. The ring finger showed a much lower heat flux than the other digits, indicating it was typically not making as good contact with the grasp object. Future development of the test procedure could be devised to further reduce the uneven distribution and provide more accurate data. Despite nonuniform contact, analysis was still able to compute conductances on locations of the glove where high quality contact was made.

4. Chamber Pressure

Following testing, data analysis showed better performance of the gloves at the coldest test point (48K) than the other temperature test points. Ultimately, this finding led to the discovery of chamber pressure inconsistencies at the higher test points. At test points warmer than 48 K, the chamber was not maintaining a high-quality vacuum, with pressures generally around ~1 torr. This elevated pressure is sufficient to cause significant degradation of the thermal insulation performance of the gloves. Specifically, the presence of gas between the layers of insulation reduces the effectiveness of the glove's multi-layer insulation (MLI), increasing heat transfer across the MLI layers. Additionally, higher chamber pressure enhances natural convection and conduction on the outer surface of the glove, further compromising its thermal protection. Lastly, the elevated pressure decreases the thermal contact resistance between the glove and the grasp object, facilitating greater heat transfer at points of contact.

Ultimately, the elevated chamber pressure had substantial impacts on the performance of the gloves. Through model correlation efforts, it was determined that the differences in performance between the gloves at the 48 K test points and the warmer test points was of comparable magnitude to the effects of the degraded vacuum. Thermal models were also correlated with and without the impacts of this non-ideal vacuum to estimate the expected performance of the gloves at the warm temperatures where the chamber did not maintain a high quality vacuum. Due to the poor vacuum at the warmer test points, the conductances and all analysis was based on the 48K test points in the test matrix since these test points maintained a high quality chamber pressure ($<10^{-3}$ torr). More details on the impacts of chamber pressure can be found in the final NASA Engineering and Safety Center (NESC) report on this task.[5]

C. Transient Plots

The large case matrix of this test series resulted in the generation of hundreds of transient plots. Figure 4 shows an example of a typical transient plot for discussion. The NESC report on this analysis should be referenced for all other plots. Figure 4 shows the temperatures of the hand (solid black line), restraint (dotted black line), external TMG (dashed black line) and hand heat flux (blue line) on four fingers. At the start of each test point, the heat flux rapidly increases while all temperatures decrease. The magnitude of the heat flux highlights the difference in contact across the four fingers. The ring finger has a lower heat flux indicating less contact with the grasp object on the ring finger. The transient plots also show that a steady state condition was approached, but not met, for the temperatures and heat fluxes. Steady state conditions were generally not met because the test points were terminated prior to steady state to

protect the integrity of the hand and glove (avoiding minimum permissible temperatures). Exponential extrapolation was needed to predict the steady state conditions of the finger and glove.

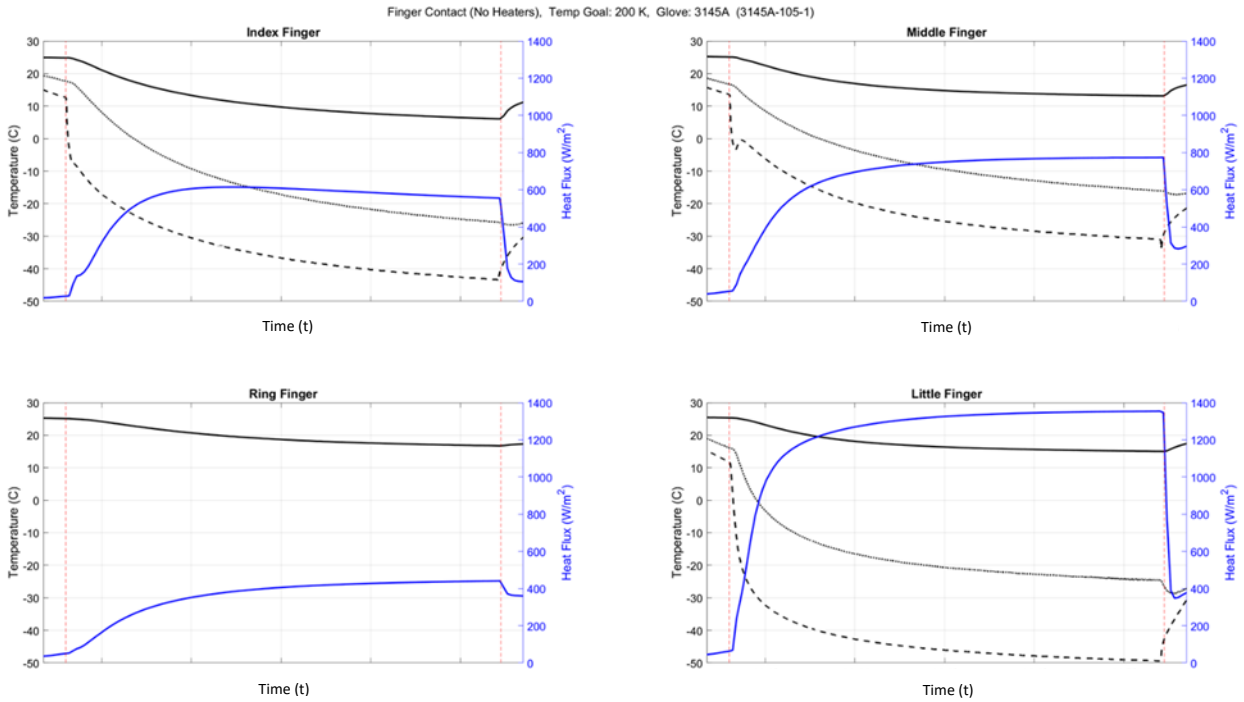


Figure 4. Transient plots of temperatures and heat flux on the fingers for a finger contact test point at a grasp temperature of 200 K.

Figure 5 shows the resultant temperatures and heat fluxes at the palm of the glove during a palm contact case. Note that the magnitude of the heat flux is much lower at the palm locations when compared to the finger contact conditions in the previous figure. This indicates that there is significantly better insulation in the glove at the palm than the fingertips. This is likely due to the presence of the palm bar, a metal support bar in the palm of the glove which prevents the palm from compressing all of the glove layers at the palm. This is also likely due to the increased surface area on the fingers when compared to the palm.

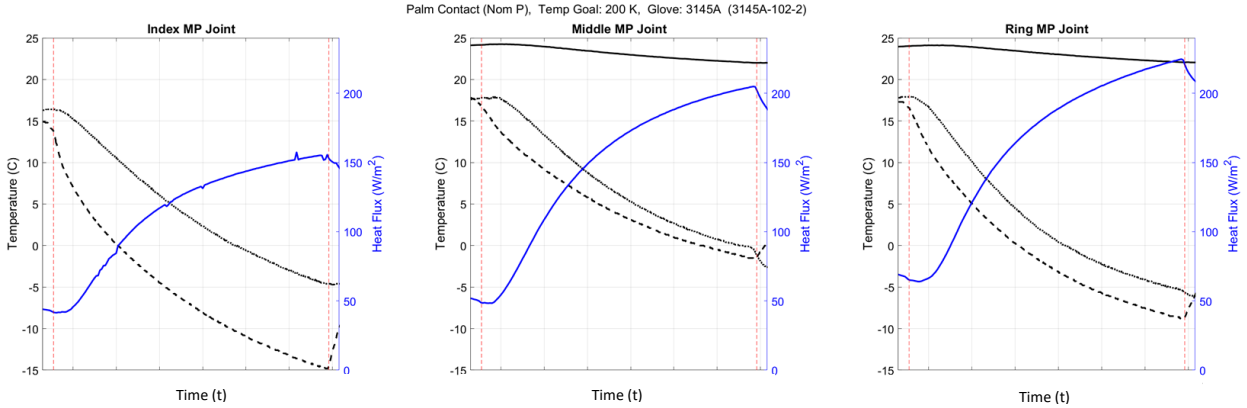


Figure 5. Transient plots of temperatures and heat flux on the palm for a palm contact test point at a grasp temperature of 200 K.

D. Analysis of Conductances

The conductances of the various layers of the glove were computed and used to compare the performance of the different glove types (3145 vs 157 TMG), repeatability of the test setup (3145A vs 3145B), and contact pressure. Comparing the conductances allows for the thermal performance of the glove to be compared across many different test points with different test durations and initial conditions.

Conductances with the 3145 and 157 TMG were compared to assess a potential difference in performance of the gloves. To compare the gloves, a two sample *t*-test was conducted. This test showed that, at a 95-percent confidence level, there are no statistical differences in the conductance between the 3145 TMG and 157 TMG.

The conductances of the two 3145 gloves were also compared and similarly showed no differences in performance. This shows that the test is repeatable and there was no significant difference in the performance of two different glove articles of the same type.

Lastly, the conductances were used to assess the impact of contact pressure. The palm contact cases were conducted with two separate contact pressures. Ultimately, this comparison showed no difference between the conductances at different pressures indicating that the insulation of the glove (at the palm) does not appear to depend on the contact pressure. This is likely due to the metal palm bar in the glove, which prevents compression of the hand into the glove at higher pressures. It is likely that if contact pressure was varied at the finger locations, a bigger impact would have been observed due to lack of a palm bar, although this would need to be verified in future testing.

E. Prediction of Glove Performance

The goal of this test series was to assess the permissible exposure time of the glove in operational conditions. To quantify this time, the thermal model of the glove was used to compute glove curves. These curves represent the permissible exposure time to either a radiation environment or contact exposure. The glove curves are generated by running the model with various environment (for radiation) or grasp object (for contact) temperatures and determining the time for the skin to reach a temperature of 10°C (50°F). For all cases (contact and radiation only) the limiting location on the hand was the fingertips, which reached this limit first. The glove curves were computed using the same methodology developed during initial development of gloves in the 1990s.[1,4] For generation of the radiation curve, the thermal model is initialized by exposing the glove to a radiative temperature of 35°F (1.7°C) for two hours. This is assumed to represent a long duration spent in a cold airlock prior to exiting into the relevant environment. For contact cases, the model is initialized with the fingertips of the hand at a temperature of 57°F (13.9°C). This is to simulate a condition where a crewmember has cold fingers and grasps a cold object. Note that all of the contact curves assume contact with the front side of the glove. Incidental contact on the backside of the hands was not assessed in this study. Incidental content on the backside of the hand would likely have a lower permissible contact limit since this portion of the glove lacks RTV and is primarily designed for providing insulation in a radiation environment (no contact).

Figure 6 shows the glove curves for a radiation only environment and grasping conditions (with and without heaters). The dashed lines indicate data from the original Phase VI glove curve development[1] in 1998. Note that the dashed lines only span to –200°F (144 K) since the original testing of Phase VI gloves did not achieve the extreme cold temperatures from this test series. The solid lines indicate the updates to glove curves based on data from this test series.

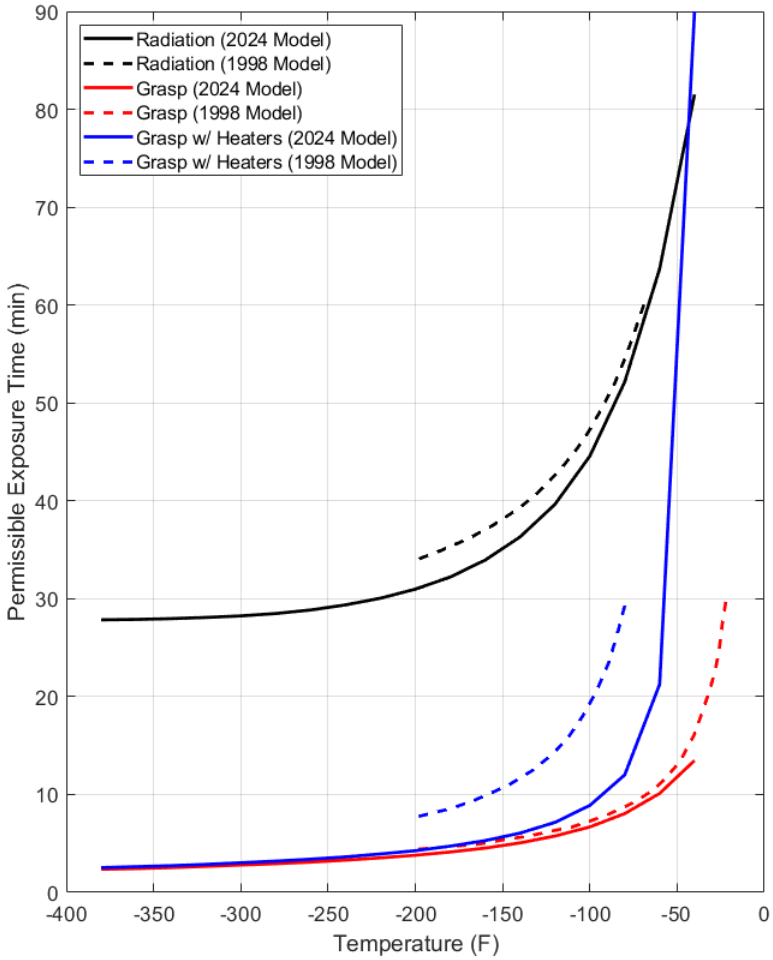


Figure 6. Glove curves for radiation only, grasping without heaters, and grasping with heaters.

The updated glove curve for radiation tracks similarly to the previous 1990s model. The permissible exposure time is slightly lower than the previous model and the gap appears to increase slightly at colder temperatures. As the temperature gets colder, the permissible exposure time for radiation contact appears to level out. This is because the primary heat transfer mechanism is due to radiation, which depends on the difference in temperatures to the fourth power. At extremely cold temperatures, the radiation heat transfer is dominated by the warm hand temperature so changes in the environment temperature only have small impacts on the heat transfer.

The grasp condition without heaters (red) does not show alignment with the 1990s model. The permissible temperature at the coldest temperatures is less than 3 minutes. Contrary to the radiation case, for contact conditions, the permissible temperature continues to decrease as temperatures get colder. This is due to the conduction heat transfer that scales proportionately to the temperature (not temperature to the fourth power). This means that the impact of the contact temperature is slightly more significant at coldest temperatures.

The grasp condition with heaters (blue) shows the largest deviations from the 1990s model. The current model shows a significantly degraded performance of the heaters when compared to the previous model. This was found to be due to issues in the old thermal model, which inaccurately assumed heaters provided heat around the full circumference of the fingertips and fingers. In reality, the heaters are only located on the backside of the fingertips. This results in a limited ability in the gloves to maintain a warm temperature on palm side of the fingertips when contacting a cold grasp object. Conduction from the fingertip to the cold object dominates the system, and the heat injected on the backside of the fingertips does not have sufficient thermal pathways to rapidly warm the palm side of the fingertips. While these curves do not show a substantial improvement in performance from the heaters, it is important to recall the assumptions built into the generation of these curves. The glove curves are based on assuming

the fingertips start at an already cold temperature of 57°F (13.9°C). During operation, the heaters would hopefully be turned on prior to the fingertip temperatures reaching these cold temperatures, which would give the heat from the heaters more time to warm the full fingertips.

V. Summary of Analysis and Testing

The findings of this study provide critical insights into the thermal performance of the Phase VI glove under various conditions and environments. The highest heat fluxes were observed at the fingertips and fingers of the gloves, indicating poorer insulation in these areas compared to the palm of the glove. This highlights the need for enhanced thermal protection in the finger regions to ensure better insulation performance.

The Phase VI glove palm bar, located at the MP joint, serves as a thermal barrier, resulting in comparable insulation performance for both radiation and contact cases. This structural feature underscores the importance of the palm bar in maintaining thermal consistency across different exposure scenarios. Additionally, despite being constructed with different RTV materials, there is no statistical difference in the conductance values of the 157 and 3145 gloves at 48 K, suggesting that the choice of RTV material does not significantly impact thermal conductance at ultra-cold temperatures.

In radiation-only environments, differences in maximum predicted exposure times between the 1990s and updated Phase VI glove thermal models increase as temperatures decrease, but these differences never exceed approximately 3 minutes. This indicates that both models remain consistent in their predictive capabilities, with only minor variations under these conditions. The updated thermal model predicts a minimum permissible exposure time of approximately 28 minutes in lunar south pole PSRs, reflecting the model's improved accuracy and applicability to extreme lunar environments.

For grasping conditions without heaters, the maximum predicted contact time differences between the 1990s and updated Phase VI glove thermal models never exceed 4 minutes, suggesting that both models provide consistent predictions in these scenarios. However, with heaters activated, the updated thermal model predicts significantly shorter durations than the 1990s model, primarily due to the corrected placement of the heat source on the backside of the fingertips. Despite this adjustment, the fingertip heaters in the Phase VI glove do not significantly improve the permissible contact duration when grasping objects at temperatures representative of lunar south pole PSRs, highlighting the need for further optimization of the heating system.

These findings emphasize the importance of targeted thermal enhancements in specific areas of the glove and the need for continued refinement of thermal models to improve the performance and safety of EVA gloves in extreme environments.

VI. New ASTM Standard Formation

As part of this assessment, it was the desire of the NASA team to capture the modified method for evaluating the thermal response of an EVA glove. Therefore, similar to the other tasks conducted for this effort, this procedure will be submitted to the ASTM.

A request to create a standard was submitted through the cross-cutting subcommittee within the ASTM F47 Committee on Commercial Spaceflight. No objections to having that standard within this subcommittee were present so an ASTM work item was generated. ASTM WK85993 for the development of a new "Measuring the Radiant and Contact Conductance of Glove Assemblies Worn on Extravehicular Activities" is now allowed to be developed and submitted through the ASTM process.

Once the method is fully developed and balloted the members of the ASTM F47.05 subcommittee on crosscutting will vote on the technical content within the standard. If anyone reading the ballot disagrees with the content, then they are allowed to vote negative. All negative votes are reviewed and discussed by the subcommittee members made up of end users, manufactures, and general interest participants. They vote to determine if the negative is considered persuasive or not. If the negative is found persuasive, then the author of the ballot is asked to go back and make revisions and resubmit through the balloting process again. This continues until no negatives are received or all negatives are found non-persuasive at the subcommittee level.

Once the ballot of the method passes the subcommittee it must then be balloted throughout the entire ASTM F47 committee. The process is the same as at the subcommittee level. Once the standard is balloted and no negatives are found, or all negatives are found non-persuasive, the standard passes and is sent to the ASTM Committee on Standards (COS) for final approval. The role of the COS is to make sure all processes were followed before issuing and printing it as an official ASTM standard.

VII. Conclusion

This Task was aimed at the creation of a novel standardized test protocol for characterizing the thermal performance of a glove assembly and then using that procedure to collect glove data at temperatures equivalent to lunar PSR. A NASA-developed test method was established using a thermally controlled manikin hand, THS, outfitted with a suite of sensors. The glove is installed over the hand and both items are inserted into a thermal vacuum chamber capable of achieving 48 K. When defined temperature set points are achieved, extendable rods are used to manipulate the THS/glove system into the chamber where it is pressed into a thermally conditioned grasp object on the floor of the chamber. Using embedded sensors (heat flux and temperature), the procedure is utilized to collect data on the glove (in this instance, Phase VI) performance. For this task, the data were used to correlate an existing thermal math model of the glove. The math model is used to generate touch limiting temperature curves for the entire range of temperatures that could be encountered during an Artemis EVA. The curves were updated based on collected data. A statistical analysis was conducted to quantify the variability in the test.

The newly defined standardized test protocol and the data it produced constitute a portion of the total dataset of this effort. Both the amassed information and the newly established standardized tests will be shared with suit vendors and the broader community. This dissemination aims to facilitate informed decisions in EVA glove fabric selection and support future research endeavors in this critical domain.

Acknowledgments

The authors would like to thank all the various people who contributed significantly to this NESC effort, without which it would not have been successful. Special thanks to Joe Settles and Bryan Kanne (JSC-AML), for his behind the scenes work of getting so much testing completed; to Joseph Kosmo, for his development of the tumbler test and insights he provided; and to William Spenny (NESC Affiliate), for his years of experience and mentorship.

References

[1]Langston, N. L. and Margiott, V., "EMU Phase VI Glove Thermal Vacuum Test and Analysis Final Report," CTSD-SS-1621, JSC 39116, August 20, 1998.
[2]Cross-Program Design Specification for Natural Environments (DSNE), SLS-SPEC-159.
[3]NASA, "Exploration EVA System Destination Environments Specifications," EVA-EXP-0039, 2020.
[4]Bue, G. C., "Shuttle EMU 4000 Series and 4750 Series Glove Thermal Performance Test Final Report," CTSD-SH-898, *Crew and Thermal Systems Division*, 10 Nov. 1994.
[5]Abney, M., et al., "NASA Engineering and Safety Center Technical Assessment Report: Lunar Glove Thermal and Durability Analysis, Test, and Failure Mitigation," TI-21-01722, Sept 2024.